Available online at www.sciencedirect.com

ScienceDirect

Virology 353 (2006) 133–143

VIROLOGY

www.elsevier.com/locate/yviro

Characterization of mimivirus NAD$^+$-dependent DNA ligase

Delphine Benarroch, Stewart Shuman *

Molecular Biology Program, Sloan-Kettering Institute, New York, NY 10021, USA

Received 7 March 2006; returned to author for revision 6 April 2006; accepted 7 April 2006
Available online 14 July 2006

Abstract

Mimivirus, a parasite of *Acanthamoeba polyphaga*, is the largest DNA virus known; it encodes a cornucopia of proteins with imputed functions in DNA replication, modification, and repair. Here we produced, purified, and characterized mimivirus DNA ligase (MimiLIG), an NAD$^+$-dependent nick joining enzyme homologous to bacterial LigA and entomopoxvirus DNA ligase. MimiLIG is a 636-aa polypeptide composed of an N-terminal NAD$^+$ specificity module (domain Ia), linked to nucleotidyltransferase, OB-fold, helix–hairpin–helix, and BRCT domains, but it lacks the tetracysteine Zn-binding module found in all bacterial LigA enzymes. MimiLIG requires conserved domain Ia residues Tyr36, Asp46, Tyr49, and Asp50 for its initial reaction with NAD$^+$ to form the ligase–AMP intermediate, but not for the third step of phosphodiester formation at a preadenylylated nick. MimiLIG differs from bacterial LigA enzymes in that its activity is strongly dependent on the C-terminal BRCT domain, deletion of which reduced its specific activity in nick joining by 75-fold without affecting the ligase adenylylation step. The ΔBRCT mutant of MimiLIG was impaired in sealing at a preadenylylated nick. We propose that eukaryal DNA viruses acquired the NAD$^+$-dependent ligases by horizontal transfer from a bacterium and that MimiLIG predates entomopoxvirus ligase, which lacks both the tetracysteine and BRCT domains. We speculate that the dissemination of NAD$^+$-dependent ligase from bacterium to eukaryotic virus might have occurred within an amoebal host.

Keywords: Mimivirus; Entomopoxvirus; BRCT domain; Gene transfer

Introduction

DNA ligases are found in all free-living organisms and are essential for the maintenance of cellular genome integrity (Lehman, 1974). They are responsible for joining Okazaki fragments on the lagging strand of the DNA replication fork and restoring continuity of the DNA backbone subsequent to nucleotide excision and base excision repair. DNA viruses, as extrachromosomal replicons, also rely on ligases to guard their genomes against breaks introduced during replication and recombination or DNA damage caused by environmental agents or genoclastic host defenses. Whereas small DNA viruses depend primarily on cellular enzymes for their replication and repair, many of the larger DNA viruses encode their own enzymatic machinery for viral DNA transactions, often including a viral DNA ligase. The bacterial DNA viruses T4 and T7 were among the original sources for discovery of DNA ligases in 1967 (Weiss and Richardson, 1967; Becker et al., 1967), and these bacteriophage ligases have figured prominently in the elucidation of the ligase catalytic mechanism and protein structure (Weiss et al., 1968; Harvey et al., 1971; Subramanya et al., 1996). Several eukaryotic virus-encoded DNA ligases have also been characterized biochemically or structurally, including the ligases of poxviruses (Kerr and Smith, 1989; Shuman and Ru, 1995; Shuman, 1995; Sekiguchi and Shuman, 1997; Sriskanda et al., 2001; Lu et al., 2004), baculovirus (Pearson and Rohrmann, 1998), African swine fever virus (Hammond et al., 1992; Lamarche et al., 2005), and *Chlorella* virus (Ho et al., 1997; Sriskanda and Shuman, 1998, 2002a,b; Odell et al., 2000).

Nick sealing by all DNA ligases occurs via a series of three nucleotidyl transfer reactions (Lehman, 1974). In the first step, a lysine nucleophile in the ligase active site attacks the α phosphorus of ATP or NAD$^+$ to form a covalent lysyl–N-AMP intermediate and expel either pyrophosphate or nicotinamide mononucleotide (NMN). In the second step, the 5′ phosphate of the DNA nick attacks the phosphorus of lysyl–AMP to form a DNA–adenylylate intermediate [A(5′)pp(5′)DNA] and expel the lysine. The third step is the attack of the nick

* Corresponding author.
E-mail address: s-shuman@ski.mskcc.org (S. Shuman).

0042-6822/$ - see front matter © 2006 Published by Elsevier Inc.
doi:10.1016/j.virol.2006.04.032

3′-OH on the DNA–adenylylate to form a 3′–5′ phosphodiester and release AMP.

NAD^+-dependent and ATP-dependent DNA ligases comprise two distinct branches of the covalent nucleotidyltransferase superfamily, which includes RNA ligases and mRNA capping enzymes (Shuman and Lima, 2004). The superfamily members catalyze chemically similar NMP addition reactions at polynucleotide 5′ ends via lysyl–NMP intermediates. DNA ligases and RNA capping enzymes contain two structural modules that comprise a catalytic core: a proximal nucleotidyltransferase (NT) domain and a distal OB-fold (OB) domain (Subramanya et al., 1996; Odell et al., 2000; Pascal et al., 2004; Håkansson et al., 1997; Fabrega et al., 2003; Singleton et al., 1999; Lee et al., 2000; Gajiwala and Pinko, 2004; Srivastiva et al., 2005) (Fig. 1A). Structure–function analyses have pinpointed five conserved peptide motifs (I, III, IIIa, IV, and V; see Fig. 1B) within the NT domain that comprise the NMP-binding pocket (Shuman and Lima, 2004).

The ATP-dependent DNA ligases are found in all three phylogenetic domains of cellular life: bacteria, archaea and eukarya (Martin and MacNeill, 2002; Cheng and Shuman, 1997; Sriskanda et al., 2000; Keppetipola and Shuman, 2005). In contrast, the NAD^+-dependent ligases, exemplified by the founding member *Escherichia coli* LigA (Zimmerman et al., 1967; Olivera and Lehman, 1967), have been regarded as unique to bacterial cells. LigA proteins are composed of six structural modules: N-terminal domain Ia, the NT and OB domains, a tetracysteine Zn-binding domain, a helix–hairpin–helix (HhH) domain, and a C-terminal BRCT domain (Fig. 1A). (The BRCT domain is a structural motif named for the C-terminal domain of the breast cancer susceptibility gene product BRCA1.) An NAD^+-dependent LigA enzyme is found in every known

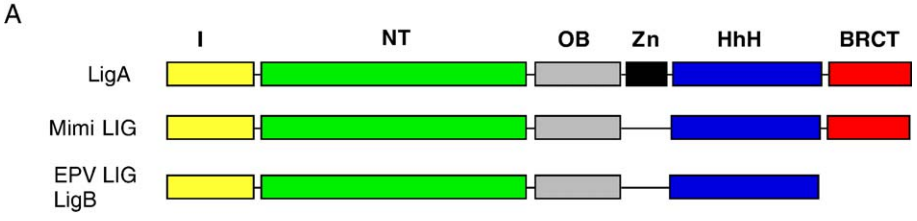

B

```
Mimi    LNATDIEEALSVSSEYYHNTGTSLISDQEYDILMDRLKELNPSSKIFAQVGAPVK-----  74
EcoA    QQLTELRTTLRHHEYLYHVMDAPEIPDAEYDRLMRELRELETKHPELITPDSPTQRVGAA  65

Mimi    ----GKKVKLPFWMGSMNKIKADE------KAVNKWL-NEYSGPYVISDKLDGISCLLTI  123
EcoA    PLAAFSQIRHEVPMLSLDNVFDEESFLAFNKRVQDRLKNNEKVTWCCELKLDGLAVSILY  125

Mimi    KNN-KTKLYTRGDGTYGQDITHLLGLINIDIGLL--EEIDQDIAIRGELIMSKKNFEKYQ  180
EcoA    ENGVLVSAATRGDGTTGEDITSNVRTIRAIPLKLHGENIPARLEVRGEVFLPQAGFEKIN  185

Mimi    E--------IMANARNMVGGIVNSKPESVNKDHAADVDLIFYEVIKP-----NDKLSRQL  227
EcoA    EDARRTGGKVFANPRNAAAGSLRQLDPRITAKRP--LTFFCYGVGVLEGGELPDTHLGRL  243

Mimi    KILKEWGLKVVYY--NIYKTFDVNILESVLSERKKKSGYEIDGIIVTDNNKHVRNISG--  283
EcoA    LQFKKWGLPVSDRVTLCESAEEVLAFYHKVEEDRPTLGFDIDGVVIKVNSLAQQEQLGFV  303

Mimi    --NPSYSFAFKGDTPTIDTVVKRVIWTPSKDGVLVPRIKFKKVRLSNVDLEYTTGFNAKY  341
EcoA    ARAPRWAVAFKFPAQEQMTFVRDVEFQVGRTGAITPVARLEPVHVAGVLVSNATLHNADE  363

Mimi    IVDNKIGSGAIINVVRSGDVIPYITHVVKPAKKPDLPNIEYVWDKNGVNIILADINDNET  401
EcoA    IERLGLRIGDKVVIRRAGDVIPQVVNVVLSERPEDTREVVF---PTHCPVCGSDVERVEG  420

Mimi    VIIKRLT--------------KFM--RNIGAENISEGITTRLVEAGFDTIP-KIINMTEE  444
EcoA    EAVARCTGGLICGAQRKESLKHFVSRRAMDVDGMGDKIIDQLVEKEYVHTPADLFKLTAG  480

Mimi    DFLTIDGFQERLAEKIYNNLQNSLDNLDILTLMDASNIFG-RGFGTKKFKKILDVYPNIV  503
EcoA    KLTGL----ERMGPKSAQNVVNALEKAKETTFARFLYALGIREVGEATAAGLAAYFGTLE  536

Mimi    NQYTKETDNIWRKKLLDIEGFDTITVNKFLGEMPNFQKFYKVINKTITIKP--YISEVNS  561
EcoA    ALEAASIEEL--QKVPDVGIVVASHVHNFFAEESNRNVISELLAEGVHWPAPIVINAEEI  594

Mimi    EGIFQNQTVVFTG----FRNADWQKFIENEGGKVSGSVSKNTSLLVYNDGEESSAKYQKA  617
EcoA    DSPFAGKTVVLTGSLSQMSRDDAKARLVELGAKVAGSVSKKTDLVI--AGEAAGSKLAKA  652

Mimi    KQLGIKTMTKSSFSKKFEK*  636
EcoA    QELGIEVIDEAEMLRLLGS*  671
```

Fig. 1. Conservation of domain structure and amino acid sequence between MimiLIG and bacterial LigA. (A) Comparison of the domain structures of bacterial LigA, MimiLIG, entomopoxvirus (EPV) ligase, and bacterial LigB. Domain Ia is an NMN-binding module found in all NAD^+-dependent DNA ligases. See text for details. (B) The amino acid sequence of MimiLIG is aligned to that of *E. coli* LigA. The polypeptide segments corresponding to the structural domains are shaded as follows: domain Ia (yellow); nucleotidyltransferase (green); OB-fold (gray); HhH (blue). The conserved nucleotidyltransferase motifs are highlighted in boxes within the green segment. The four Zn-binding cysteine residues that are found in LigA, but not in MimiLIG are highlighted in orange boxes. Amino acids Tyr36, Asp46, Tyr49, and Asp50 in domain Ia of MimiLIG that were targeted for alanine scanning are denoted by | above the alignment. Gaps in the alignment are indicated by dashes, and the carboxyl termini are denoted by asterisks.

bacterial proteome and LigA is essential for bacterial viability in every case tested (Wilkinson et al., 2001; Gottesman et al., 1973; Konrad et al., 1973; Park et al., 1989; Petit and Ehrlich, 2000; Kaczmarek et al., 2001; Gong et al., 2004). However, a recent study shows that the archaeon *Haloferax volcanii*, which has an ATP$^+$-dependent ligase (as do all archaea), also has an NAD$^+$-dependent ligase, the first such sighting in a free-living organism outside the bacterial domain of life (Zhao et al., 2006). Moreover, neither of the *Haloferax* ligases is essential for viability because they are functionally redundant, that is, the genes encoding the ATP- and NAD$^+$-dependent ligases can be deleted singly, but not in combination (Zhao et al., 2006). The *Haloferax* NAD$^+$-dependent ligase is structurally homologous to bacterial LigA proteins. A phylogenetic sequence comparison hints that *Haloferax* might have acquired its NAD$^+$-dependent ligase by horizontal gene transfer from a δ-proteobacterium.

Until recently, it was thought that viral DNA ligases were all of the ATP-dependent variety, as is the case for the ligases of T4, T7, vaccinia, baculovirus, and African swine fever virus. This presumption was overturned by the discovery and characterization of the NAD$^+$-dependent DNA ligases of the *Amsacta moorei* and *Melanoplus sanguinipes* entomopoxviruses (Sriskanda et al., 2001; Lu et al., 2004). The entomopoxvirus ligases are structurally homologous to bacterial LigA, although they lack the tetracysteine and BRCT domains. The fact that invertebrate poxviruses have an NAD$^+$-ligase (which is not found in any eukaryotic organism), while mammalian poxviruses like vaccinia have an ATP-dependent ligase that is highly homologous to mammalian DNA ligase III, raises interesting questions about where the entomopoxviruses might have acquired their NAD$^+$-dependent ligase genes. Another arthropod virus, *Chilo* iridescent virus (a member of the Iridovirus family), encodes a LigA-like polypeptide (Jakob et al., 2001), but its activity and substrate specificity have not been tested biochemically.

Mimivirus is a recently identified parasite of *Acanthamoeba polyphaga* that has an extraordinarily large genome (1.2 Mb) encoding 911 predicted proteins (44). The mimivirus proteome embraces a slew of proteins with imputed functions in DNA metabolism, including two DNA polymerases, a PCNA sliding clamp, three DNA topoisomerases (types IA, IB and II), and an NAD$^+$-dependent DNA ligase (Raoult et al., 2004). Characterization of the mimivirus type IB topoisomerase (MimiTopIB) shows it to be a structural and functional homolog of poxvirus TopIB and the poxvirus-like TopIB enzymes found in many bacteria (Benarroch et al., 2005). Based on its DNA cleavage site specificity, MimiTopIB is functionally more akin to poxvirus TopIB than bacterial TopIB, despite its greater primary structure similarity to the bacterial TopIB group. These results suggested the occurrence of TopIB gene transfer between bacteria, mimivirus, and poxviruses.

Here we purify and characterize the mimivirus DNA ligase (henceforth named MimiLIG). We find that MimiLIG is a bona fide nick sealing enzyme with specificity for NAD$^+$ as its nucleotide substrate. Although biochemically similar to bacterial LigA, MimiLIG lacks the tetracysteine Zn-binding module found in all LigA enzymes. MimiLIG exemplifies an intermediate evolutionary stage between LigA and the NAD$^+$-dependent entomopoxvirus DNA ligases with respect to its protein domain composition. Our results suggest that dissemination of NAD$^+$-dependent ligases from bacteria to eukaryal viruses occurred by horizontal transfer, perhaps in an ancestral amoebal host.

Results

A mimivirus protein related to NAD$^+$-dependent DNA ligases

Bacterial LigA, the prototypal NAD$^+$-dependent ligase found in all bacteria, is composed of a central ligase core (the NT and OB domains) flanked by an N-terminal module (domain Ia) and three C-terminal modules, including a tetracysteine domain that binds a single Zn atom, a helix–hairpin–helix (HhH) domain, and a BRCT domain (Singleton et al., 1999; Lee et al., 2000; Gajiwala and Pinko, 2004; Srivastiva et al., 2005) (see Fig. 1). Domain Ia confers NAD$^+$ specificity via interaction with the NMN moiety of NAD$^+$ (Sriskanda et al., 2001; Gajiwala and Pinko, 2004; Sriskanda and Shuman 2002c). Several species of bacteria have a second NAD$^+$-dependent DNA ligase (LigB) in addition to LigA (Sriskanda and Shuman, 2001). The LigB proteins contain the Ia, NT, OB, and HhH domains, but lack the C-terminal BRCT domain and two of the four Zn-binding cysteines found in LigA (Fig. 1A). The two entomopoxvirus NAD$^+$-dependent DNA ligases are composed of Ia, NT, OB, and HhH domains; they are missing the tetracysteine and BRCT modules (Sriskanda et al., 2001; Lu et al., 2004) (Fig. 1A). Here we focus on the mimivirus R303 gene product (MimiLIG), a 636-aa polypeptide that displays primary structure similarity to bacterial and entomopoxvirus NAD$^+$-dependent DNA ligases (Fig. 1). MimiLIG is composed of Ia, NT, OB, HhH, and BRCT domains. The primary structure alignment of MimiLIG and *E. coli* LigA shown in Fig. 1B highlights conservation of the nucleotidyltransferase motifs that form the AMP binding pocket (green boxes) and the identity of the four amino acids of domain Ia that comprise the NMN binding site (denoted by |). All four Zn-binding cysteines of *E. coli* LigA are absent in MimiLIG (Fig. 1B).

Recombinant MimiLIG is an NAD$^+$-dependent nick sealing enzyme

MimiLIG was produced in *E. coli* as a His$_{10}$-Smt3 fusion and purified from a soluble bacterial lysate by Ni^{2+}-agarose chromatography. The His$_{10}$-Smt3 tag was removed by the Smt3-specific protease Ulp1, and the tag-free MimiLIG was separated from the tag by a second step of Ni^{2+}-agarose chromatography. SDS-PAGE showed that the preparation consisted of a major 70 kDa polypeptide corresponding to MimiLIG (Fig. 2A, WT).

Recombinant MimiLIG protein sealed a singly nicked duplex DNA substrate in the presence of NAD$^+$ and magnesium, converting 94% of the input 5′ 32P-labeled 18-mer strand into a labeled 36-mer product (Fig. 2B, lane WT). The extent of nick sealing in the presence of 50 μM NAD$^+$ was proportional to the amount of MimiLIG added (Fig. 3A). From the slope of the titration curve, we estimate that >100 fmol of

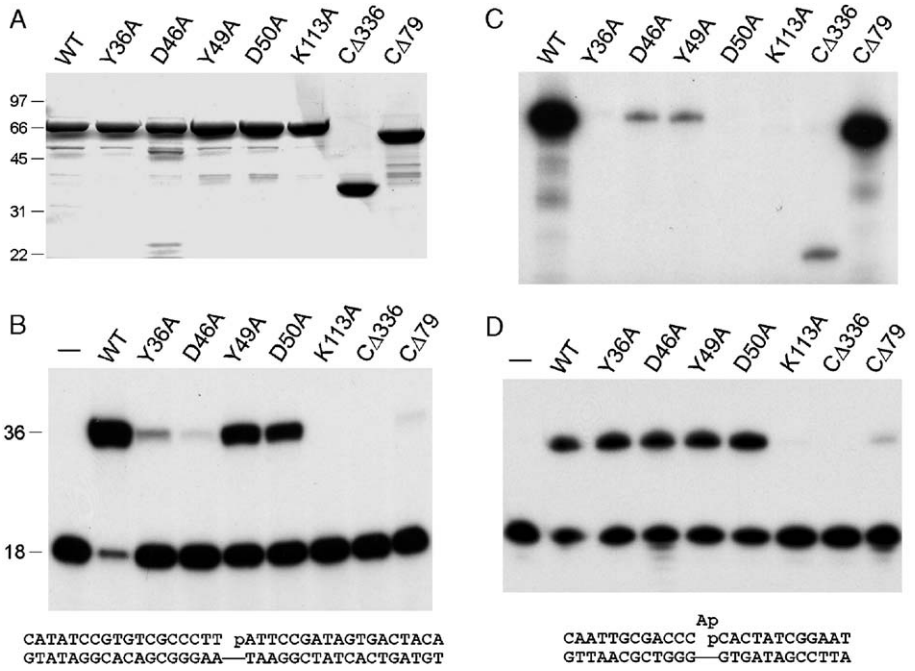

Fig. 2. Purification and activities of wild-type MimiLIG and MimiLIG mutants. (A) Aliquots (5 μg) of wild-type MimiLIG, the indicated Ala mutants, and the CΔ336 and CΔ79 truncation variants were analyzed by SDS-PAGE. Polypeptides were visualized by staining with Coomassie blue dye. The positions and sizes (kDa) of marker polypeptides are indicated on the *left*. (B) Nick joining reaction mixtures (20 μl) containing 50 mM Tris–HCl (pH 7.5), 10 mM $(NH_4)_2SO_4$, 5 DTT, 5 mM $MgCl_2$, 50 μM NAD^+, 1 pmol ^{32}P-labeled nicked DNA, and 20 fmol of the specified MimiLIG preparation were incubated for 30 min at 37 °C. The reaction products were resolved by PAGE and visualized by autoradiography. MimiLIG was omitted from the control reaction shown in lane –. The structure of the singly nicked 36-mer DNA is illustrated at the *bottom* with the radiolabeled nick 5′-phosphate indicated by p. (C) Ligase adenylylation reaction mixtures (20 μl) containing 50 mM Tris–HCl (pH 7.5), 5 mM DTT, 5 mM $MgCl_2$, 1 μM [^{32}P-AMP]NAD^+, and 8 pmol of the specified MimiLIG preparation were incubated at 37 °C for 10 min. The products were analyzed by SDS-PAGE and visualized by autoradiography (D). Ligation at a preadenylylated nick. Reaction mixtures (20 μl) containing 50 mM Tris–HCl (pH 7.5), 5 mM DTT, 5 mM $MgCl_2$, 200 fmol ^{32}P-labeled nicked DNA–adenylylate substrate, and 1 pmol of the specified MimiLIG preparation were incubated at 37 °C for 5 min. The products were resolved by PAGE and visualized by autoradiography. MimiLIG was omitted from the control reaction shown in lane –. The structure of the nicked DNA–adenylylate substrate is illustrated at the *bottom*.

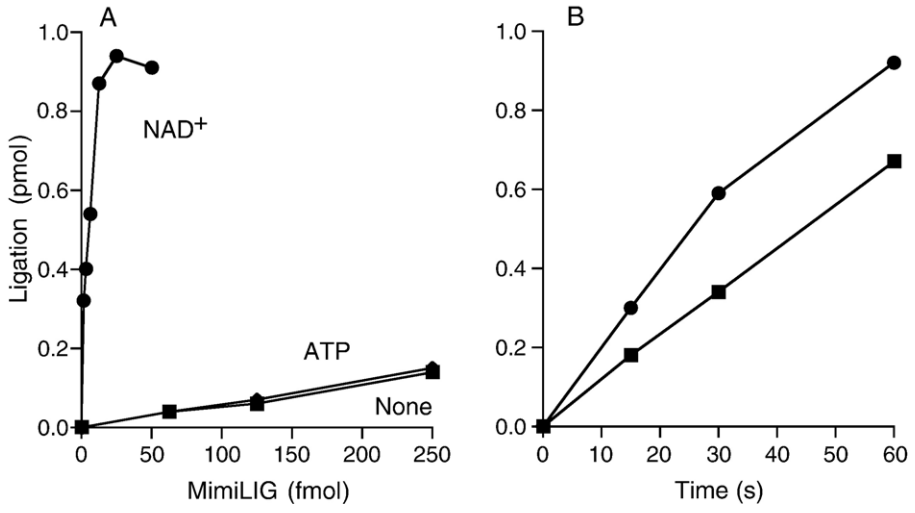

Fig. 3. Characterization of wild-type MimiLIG. (A) Nick joining reaction mixtures (20 μl) containing 50 mM Tris–HCl (pH 7.5), 10 mM $(NH_4)_2SO_4$, 5 mM DTT, 5 mM $MgCl_2$, 1 pmol 5′ ^{32}P-labeled nicked duplex DNA substrate, either 50 μM NAD^+ (●), 50 μM ATP (▲) or no added nucleotide (■), and MimiLIG as specified were incubated at 37 °C for 10 min. The extents of ligation are plotted as a function of input protein. (B) Reaction mixtures (100 μl) containing 50 mM Tris–HCl (pH 7.5), 10 mM $(NH_4)_2SO_4$, 5 mM DTT, 5 mM $MgCl_2$, 50 μM NAD^+, 5 pmol 5′ ^{32}P-labeled nicked duplex DNA substrate, and either 165 fmol (■) or 330 fmol (●) of MimiLIG were incubated at 37 °C. Aliquots (20 μl) were withdrawn at the times specified and quenched immediately with an equal volume of 95% formamide, 20 mM EDTA. The extents of ligation per sample (containing 1 pmol input substrate) are plotted as a function of time.

ends was sealed per fmol of MimiLIG. The rate of ligation in the presence of 50 μM NAD^+ was proportional to input MimiLIG (Fig. 3B). From these data, we estimated a turnover number of ~18 min^{-1}. Activity in the absence of added NAD^+, which was detectable at stoichiometric levels of enzyme to nicked DNA substrate (Fig. 3A), reflected the presence of preadenylylated MimiLIG in the enzyme preparation. The linear dependence of NAD^+-independent product formation on input enzyme indicated that ~56% of the MimiLIG molecules had AMP bound covalently at the active site. Inclusion of 50 μM ATP in lieu of NAD^+ failed to stimulate the joining reaction above the level seen in the absence of added nucleotide. Thus, MimiLIG is a bona fide NAD^+-dependent DNA ligase.

The native size of MimiLIG was gauged by zonal velocity sedimentation through a 15–30% glycerol gradient containing 0.5 M NaCl. Marker proteins catalase (248 kDa), ovalbumin (43 kDa), and cytochrome *c* (12 kDa) were included as internal standards. Aliquots of the even-numbered gradient fractions were analyzed by SDS-PAGE (Fig. 4A) and assayed for nick sealing (Fig. 4B). The 70 kDa MimiLIG polypeptide sedimented as a single component with a peak at fractions 18–20, a position just ahead of the ovalbumin peak in fraction 20. A single peak of ligase activity coincided with the distribution of the MimiLIG protein. We surmise that MimiLIG is a monomer in solution.

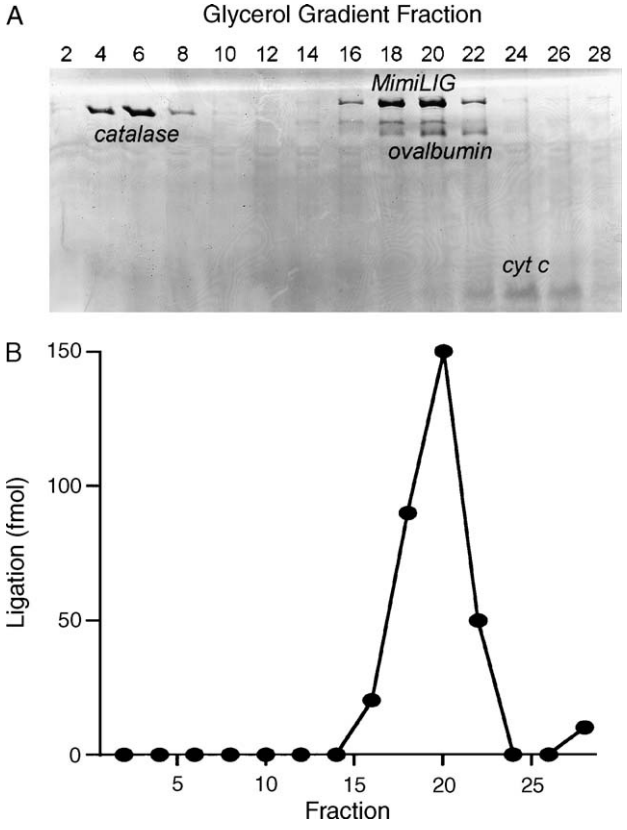

Fig. 4. Velocity sedimentation of MimiLIG. Sedimentation in a glycerol gradient was performed as described under Materials and methods. (A) Aliquots (16 μl) of the even-numbered gradient fractions were analyzed by SDS-PAGE. The Coomassie blue-stained gel shows the polypeptides corresponding to MimiLIG and the sedimentation standards catalase, ovalbumin, and cytochrome *c*. (B) Nick joining reaction mixtures (20 μl) containing 50 mM Tris–HCl (pH 7.5), 10 mM $(NH_4)_2SO4$, 5 mM DTT, 5 mM $MgCl_2$, 50 μM NAD^+, 1 pmol of 5′ ^{32}P-labeled nicked DNA, and 1 μl of a 1:100 dilution of the indicated gradient fractions were incubated for 10 min at 37 °C.

Effects of alanine mutations in domain Ia and motif I on the nick sealing activity of MimiLIG

Domain Ia is the NAD^+ specificity determinant of bacterial LigA and the *A. moorei* entomopoxvirus DNA ligase. Previous studies showed that mutations of conserved amino acids Tyr22, Asp32, Tyr35, and Asp36 within domain Ia of *E. coli* LigA either severely reduced or abolished nick sealing and adenylylate transfer from NAD^+ (Sriskanda et al., 2001; Sriskanda and Shuman, 2002c). These four side chains comprise a binding site for the NMN moiety of NAD^+ (Gajiwala and Pinko, 2004). All of the NMN-binding side chains of *E. coli* LigA are conserved in MimiLIG (Fig. 1B). To probe whether domain Ia functional groups are relevant to the activity and NAD^+ specificity of MimiLIG, we introduced single alanine substitutions at Tyr36, Asp46, Tyr49, and Asp50. We also mutated Lys113 in motif I, which is the predicted site of covalent AMP attachment in MimiLIG. The Y36A, D46A, Y49A, D50A, and K113A proteins were produced in *E. coli* and purified free of their tags in parallel with wild-type MimiLIG (Fig. 2A). Sealing activity in the presence of 50 μM NAD^+ was assayed initially at a 50:1 molar ratio of nicked DNA substrate to input enzyme, conditions that result in nearly quantitative nick closure by wild-type MimiLIG (Fig. 2B). As expected, the K113A protein was inert. The Y36A and D46A proteins displayed only trace sealing activity, whereas the Y49A and D50A mutants retained activity, albeit less than wild-type MimiLIG. The specific activities of the domain Ia mutants in the nick sealing reaction were determined by enzyme titration (not shown). The results, when normalized to the wild-type specific activity (defined as 100%), were as follows: the Y36A and D46A mutations decreased activity to <1% of wild-type; the D50A and Y49A enzymes were 2% and 6% as active as wild-type, respectively.

Mutational effects on ligase adenylylation

The first step in DNA ligation is the formation of a covalent enzyme–adenylylate intermediate (Lehman, 1974; Weiss et al., 1968; Zimmerman et al., 1967; Olivera and Lehman, 1967). Incubation of wild-type MimiLIG with 1 μM [^{32}P-AMP]NAD^+ and magnesium resulted in the formation of a ^{32}P-labeled covalent nucleotidyl–protein adduct that comigrated with the MimiLIG polypeptide during SDS-PAGE (Fig. 2C, WT). The K113A mutant protein was unreactive with [^{32}P-AMP]NAD^+, consistent with its role as the nucleophile in the adenylyltransferase reaction. Among the domain Ia mutants, Y36A and D50A were unreactive, whereas D46A and Y49A formed very low amounts of the covalent ligase–AMP intermediate (2.0 and 2.3% of the wild-type level, respectively). The observation that D50A retains some nick sealing activity (Fig. 2B) despite what appears to be a complete defect in step 1 (Fig. 2C) is probably attributable to the difference in the NAD^+ concentrations used

in the adenylyltransferase assay (1 μM) versus the ligation assay (50 μM). We surmise that Y36, D46, Y49, and D50 are critical for the autoadenylylation reaction of MimiLIG with NAD^+.

Domain Ia mutations do not affect sealing at a preadenylylated nick

The third step of the ligation pathway is the attack of the 3′-OH of the nick on the 5′-PO_4 of the DNA–adenylylate to form a phosphodiester and release AMP. We assayed step 3 of the ligation reaction using a preadenylylated nicked DNA substrate labeled with ^{32}P on the 5′-PO_4 of the DNA–adenylylate strand (Fig. 2D). Reaction of wild-type MimiLIG with the nicked DNA–adenylylate (in 5-fold molar enzyme excess) in the presence of magnesium without added NAD^+ resulted in strand closure, evinced by conversion of 40% of the input AppDNA strand to a radiolabeled 24-mer product. The Y36A, D46A, Y49A, and D50A mutants attained similar extents of ligation at the preadenylylated nick (Fig. 2D). Thus, the ablation of nick joining and ligase–AMP formation by these four mutations cannot be ascribed to a global folding defect, but instead reflects a specific requirement for domain Ia functional groups in the reaction of MimiLIG with NAD^+. We surmise that MimiLIG relies on the same NAD^+ specificity determinants as bacterial LigA and entomopoxvirus ligase.

The motif I lysine nucleophile is required for phosphodiester formation

In contrast to the benign effects of domain Ia mutations on the isolated step 3 reaction, the alanine change at Lys113 abolished sealing at a preadenylylated nick. These findings for MimiLIG are counter to those reported for several ATP-dependent DNA ligases, for which loss of the motif I lysine nucleophile did not preclude catalysis of step 3 (Sekiguchi and Shuman 1997; Sriskanda and Shuman 1998; Sriskanda et al., 2000; Akey et al., 2006). A requirement for the lysine in step 3 of the MimiLIG reaction echoes similar finding concerning *E. coli* LigA, whereby changing the lysine nucleophile to glutamine abolished sealing at a preadenylylated nick, although replacing the lysine with arginine restored step 3 activity to the wild-type level, despite the arginine mutant being completely defective in the composite nick sealing reaction and in step 1 adenylylation (Zhu and Shuman, 2005). The requirement for a positively charged motif I side chain for step 3 catalysis might be a shared characteristic of NAD^+-dependent DNA ligases that distinguishes them from the ATP-dependent enzymes.

Effects of deleting the BRCT domain of MimiLIG

The necessity and function of the BRCT domain of NAD^+-dependent DNA ligases have been debated. On the one hand, the fact that bacterial LigB enzymes and entomopoxvirus ligases have nick sealing activity, though they lack the BRCT domain (Sriskanda et al., 2001; Lu et al., 2004; Sriskanda and Shuman 2001), indicates that this structural module is not a defining requirement for NAD^+-dependent ligation. On the other hand, there have been several reports of the effects of deleting the BRCT domain of bacterial LigA proteins, which range from deleterious (Feng et al., 2004) to mild or minimal (Lim et al., 2001; Wilkinson et al., 2005; Jeon et al., 2004), depending on which LigA enzyme is being investigated.

Here we produced and purified a truncated version of MimiLIG (CΔ79), composed of residues 1–557, but lacking the C-terminal 79 amino acids that comprise the BRCT domain. The purity of the tag-free CΔ79 protein was comparable to that of wild-type MimiLIG, and it displayed the expected incremental increase in electrophoretic mobility (Fig. 2A). CΔ79 displayed extremely weak nick joining activity at a 50:1 ratio of nicked DNA substrate to enzyme (Fig. 2B); a protein titration showed its specific activity to be 1.3% of the activity of wild-type MimiLIG. These results suggest that the BRCT domain is critical for overall MimiLIG function.

The CΔ79 mutant was active in the step 1 adenylylation reaction with NAD^+ insofar as the yield of radiolabeled CΔ79–AMP adduct was 84% of that formed by wild-type MimiLIG (Fig. 2C). The nonessentiality of the extreme C-terminal segment for adenylylation is consistent with previous deletion analyses of other NAD^+-dependent DNA ligases (Timson and Wigley, 1999; Sriskanda et al., 2001; Kaczmarek et al., 2001; Lim et al., 2001; Feng et al., 2004; Leon et al., 2004; Wilkinson et al., 2005) and implicates the BRCT domain of MimiLIG in a downstream step of the ligation pathway. This inference was verified by the finding that the CΔ79 protein was impaired in step 3 sealing at a preadenylylated nick, generating only 7.5% as much ligated 24-mer product as did wild-type MimiLIG (Fig. 2D). Furthermore, the fact that CΔ79 is readily adenylylated, but formed no detectable DNA–adenylylate intermediate during the 5′-PO_4 nick ligation reaction (Fig. 2B), suggests that the missing BRCT domain is essential for step 2 of the ligation pathway.

A more extensive truncation of MimiLIG that eliminated 336 amino acids from the C-terminus (Fig. 2A) abolished overall ligation and step 3 activity. The CΔ336 mutant, which terminated at Thr300, consists solely of the Ia and NT domains. CΔ336A displayed weak reactivity with NAD^+, forming a truncated radiolabeled protein–AMP adduct to the extent of 4% of the amount seen with wild-type MimiLIG (Fig. 2C). Whereas the retention of adenylyltransferase by the isolated N-terminal Ia-NT fragment is consistent with results for other NAD^+-dependent ligases, the isolated domains of other enzymes generally retained higher levels of autoadenylylation than what we observed for MimiLIG. Conceivably, the deleted OB domain might either assist in the adenylylation reaction of the Ia-NT fragment or contribute to its folding and stability.

Discussion

Mimivirus encodes a score of proteins with imputed functions in DNA replication, modification, and repair (Raoult et al., 2004; Claverie et al., 2006). Here, we produced, purified, and characterized mimivirus DNA ligase, which we find to be a

structural and functional homolog of bacterial LigA and entomopoxvirus NAD$^+$-dependent DNA ligases. MimiLIG is the first instance of a biochemically verified NAD$^+$-dependent "eukaryotic" DNA ligase from a non-entomopoxvirus source. The putative NAD$^+$-dependent ligase encoded by *Chilo* iridescent virus has not been characterized biochemically. Given that it is a close structural homolog of MimiLIG (with 30% amino acid identity over a 614-aa polypeptide segment) and has the same domain components, we suspect that the iridovirus protein is also a legitimate nick sealing enzyme. Our studies of MimiLIG reveal fundamental similarities, but also significant differences, between members of the NAD$^+$-dependent ligase family. They also prompt speculation concerning how NAD$^+$-dependent DNA ligases might have been insinuated into the eukaryal domain via horizontal transfer.

MimiLIG versus other NAD$^+$-dependent ligases

We report that four amino acid side chains of domain Ia responsible for the reaction of LigA and entomopoxvirus ligases with NAD$^+$ to form the ligase–AMP intermediate are conserved and essential in MimiLIG. From the crystal structure of *Enterococcus* LigA bound to NMN (Gajiwala and Pinko, 2004), we predict that Tyr36 and Tyr49 in MimiLIG sandwich the nicotinamide base in a π stack, while Asp46 makes a hydrogen bond to the amide nitrogen of nicotinamide and Asp50 coordinates the ribose 2′-O.

Like other NAD$^+$-dependent ligases tested, MimiLIG requires the motif I lysine and the OB and HhH domains for the composite nick sealing reaction and for phosphodiester bond formation at a preadenylated nick. The HhH domain has been implicated as a component of an essential DNA binding surface, based on its conservation in all NAD$^+$-dependent DNA ligases and the observations that the isolated C-terminal segments of *B. stearothermophilus*, *S. aureus*, or *T. filiformis* LigA that include the tetracysteine, HhH, and BRCT domains can bind duplex DNA in an electrophoretic mobility shift assay (Timson and Wigley, 1999; Kaczmarek et al., 2001; Jeon et al., 2004). In the case of *Amsacta* entomopoxvirus DNA ligase, deletion of the C-terminal OB and HhH domains abolished ligase binding to the nicked DNA–adenylylate intermediate (Sriskanda et al., 2001). Although there is no crystal structure yet for an NAD$^+$-dependent DNA ligase bound to nicked duplex DNA, the crystal structure of human DNA ligase I (an ATP-dependent ligase) bound to a nicked DNA–adenylylate (Pascal et al., 2004) revealed a circumferential clamp binding mode, wherein a predominantly alpha-helical structural domain flanking the NT-OB core comprises the DNA binding surface on the face of the duplex away from the nick. This helical domain of human Lig1 is structurally similar to the HhH domain of the NAD$^+$-dependent ligases (Pascal et al., 2004).

MimiLIG differs from bacterial LigA in that it is missing the tetracysteine Zn-binding module located between the OB and HhH domains. In this respect, MimiLIG resembles the entomopoxvirus ligases. We find that MimiLIG displays vigorous sealing activity in vitro without a tetracysteine module. The essentiality of the Zn-binding module for bacterial LigA appears to depend on which protein is being investigated. Whereas Sriskanda et al. (1999) showed that alanine mutations at three of the four Zn-binding cysteines of *E. coli* LigA abolished its nick sealing activity in vitro and in vivo, Luo and Barany (1996) reported that three of the four cysteines of *T. thermophilus* LigA were nonessential for activity in vitro and in vivo. The fact that all bacteria have LigA proteins with the tetracysteine Zn-binding domain suggests that it could provide a functional advantage, although its role might overlap with that of one or more of the other LigA structural domains. Whether the Zn-binding domain of LigA is part of the DNA binding surface, or simply provides a structural spacer between the OB and HhH domains, remains unclear.

MimiLIG differs from several characterized bacterial LigA enzymes in that its activity is strongly dependent on the C-terminal BRCT domain, deletion of which reduced specific activity in nick joining by nearly two orders of magnitude without affecting the ligase adenylylation step of MimiLIG. The findings that the BRCT domain is important for the isolated step 3 reaction of MimiLIG, and that no DNA–adenylylate is formed when the ΔBRCT mutant is incubated with nicked DNA, implicate the BRCT domain in DNA binding, either via direct DNA contacts or indirect effects on the upstream OB and HhH domains. Direct involvement of the BRCT domain in DNA binding would be consistent with the report that the isolated BRCT module of *T. filiformis* LigA can bind DNA in the gel-shift assay (Jeon et al., 2004), even though the BRCT domain of *T. filiformis* LigA can be deleted with minimal impact on *Tfi*LigA function in vivo or in vitro. Our results for MimiLIG are compatible with the idea that LigA contacts the DNA via several of its domain modules, so that the effects of mutation or deleting any one contact module, such as the Zn-binding cysteines or the BRCT domain, might not have a great impact on ligase activity as long as the other domains are intact. By this reasoning, the acute reliance of MimiLIG on its BRCT domain could arise because MimiLIG lacks a tetracysteine Zn-binding module.

Ligase evolution and dissemination of NAD$^+$-dependent ligases to eukaryal viruses

Given the ubiquity of LigA in all bacterial proteomes, and the few examples of NAD$^+$-dependent ligases outside the bacterial niche, it is reasonable to suppose that the ensemble of Ia, NT, OB, tetracysteine, HhH, and BRCT domains represents the progenitor of the NAD$^+$-dependent ligase family as it branched off from other covalent nucleotidyltransferases. The newly discovered NAD$^+$-dependent ligase in the archaeon *Haloferax* contains the full set of structural domains found in bacterial LigA (Zhao et al., 2006) and was probably acquired by horizontal LigA gene transfer from a bacterium. An interesting question is whether such LigA transfer was directly from bacterial cell to archaeal cell or involved an intermediate carrier such as a transposon, plasmid, or virus. Although many bacteriophages encode an ATP-dependent DNA ligase, Wang et al. (2005) reported recently that the bacteriophage T5 genome

encodes a putative LigA-like NAD^+-dependent DNA ligase, albeit split into two adjacent open reading frames. The upstream ORF encodes a polypeptide consisting of Ia, NT and OB domains; the downstream ORF specified a polypeptide composed of tetracysteine, HhH, and BRCT domains. Hertveldt et al. (2005) reported the genome sequence of *Pseudomonas aeruginosa* phage EL, which encodes a putative NAD^+-dependent DNA ligase: a 656-aa single polypeptide containing all of the domain modules found in LigA. Thus, it appears likely that the acquisition of an NAD^+-dependent ligase gene by a virus is not unique to eukaryal agents, which makes it conceivable that viruses are both recipients and vectors for ligase gene dissemination.

MimiLIG appears to comprise a mesne stage in the devolution, or simplification, of the domain composition of NAD^+-dependent DNA ligases. Whereas MimiLIG lacks the tetracysteine Zn-binding site and contains a BRCT domain, the entomopoxvirus DNA ligases lack both of these components. Thus, the entomopoxvirus ligases can be viewed as more distantly devolved from the ancestral LigA enzyme, either along a sequential route via a MimiLIG-like intermediate missing only one module, or via a parallel pathway in which entomopoxviruses lost both modules in one stroke. We prefer the sequential scenario, especially because the loss of the tetracysteine Zn-binding site appears to reflect incremental missense changes rather than deletion of the entire internal polypeptide segment linking the OB and HhH domains. The incrementalist view of remodeling the tetracysteine motif is supported by the fact that bacterial LigB apparently retains two of the original four cysteines found in bacterial LigA but is nonetheless missing the entire BRCT domain (Sriskanda and Shuman, 2001). It is worth noting that MimiLIG is a much better nick sealing enzyme in vitro than are either *Amsacta* entomopoxvirus DNA ligase or *E. coli* LigB, which could be because the latter enzymes lack the BRCT domain that we show is important for MimiLIG.

Given the likelihood that eukaryal DNA viruses acquired the NAD^+-dependent ligases by horizontal transfer from a bacterium and the possibility that the MimiLIG-type domain composition is a precursor to the more stripped-down entomopoxvirus ligase structure, we speculate that the transfer from bacterium to virus might have occurred in an amoebal host. We discussed previously why Amoebae are plausible incubators for the transfer of TopIB between bacteria and eukaryotic viruses (specifically, mimivirus, and poxviruses) (Benarroch et al., 2005). In brief, free-living amoebae are ubiquitous in marine and soil environments; they congregate at biofilms or water–plant interfaces and feed on bacteria, fungi, and algae. Many bacteria have been identified that have the capacity to survive or grow within amoebae (especially in *Acanthamoeba*, from which mimivirus was isolated) and then exit after internalization (Greub and Raoult, 2004). The potential for transient coexistence within amoebae of diverse bacterial species and a eukaryal DNA virus sets the stage for the transfer of LigA to the eukaryal niche.

How then did NAD^+-dependent ligases spread to all known entomopoxviruses, but not to any known vertebrate poxviruses? Similar core gene content with respect to DNA and mRNA metabolism suggests that entomopoxviruses and mimivirus might derive from a common progenitor virus. Perhaps the progenitor had already acquired the NAD^+-dependent ligase gene from a bacterium by coexistence in a unicellular eukaryal host. Alternatively, a separate ancestral lineage of entomopoxvirus could have acquired its NAD^+-dependent ligase gene from a mimi-like virus. (Yet another formal possibility is that entomopoxviruses gained their ligases by gene transfer from a bacterium within an arthropod organism, with no connection to mimi-like viruses.) Although no poxviruses have yet been identified in primitive metazoa (below the level of arthropoda), or protozoa, or fungi, there is no reason to doubt that they are there, awaiting serendipitous discovery a la mimivirus. Given the fact that arthropods bite mammals and other vertebrates without immediately killing them, whereas the converse is generally not true, we imagine that today's vertebrate poxviruses descended from entomopoxviruses. In that case, they would have exchanged their original NAD^+-dependent ligases for the ATP-dependent ligases they now encode, which strongly resemble cellular DNA ligase III.

A tantalizing prospect is that eukaryal viruses bearing LigA-like genes might have delivered NAD^+-dependent ligases to their hosts. In metazoans, this would be of no consequence unless transfer occurred in germ cells; indeed, there is no sign yet of an NAD^+-dependent ligase in the available metazoan proteomes. The prospects for ligase gene transfer from virus to a unicellular host appear better, in principle, but most unicellular organisms that have viral pathogens (including amoebae and algae) have not yet had their genomes sequenced and annotated.

Materials and methods

T7-based vectors for expression of mimivirus DNA ligase

Oligonucleotide primers complementary to the 5′ and 3′ ends of the mimivirus R303 open reading frame (Genbank accession NC_006450) were used to PCR amplify the MimiLIG gene from a genomic DNA clone. The PCR primers were designed to introduce *Bam*HI restriction sites at the translation start codon (*GGATCC*ATG) and 3′ of the stop codon. The 1910-bp PCR product was digested with *Bam*HI and then inserted into the *Bam*HI site of the T7-based expression plasmid pET28b-His_{10}-Smt3. The resulting plasmid encodes MimiLIG fused to a leader polypeptide composed of a decahistidine tag linked to the yeast Smt3 protein. Sequencing of the entire insert of pET28b-His_{10}-Smt3-MimiLIG confirmed that no alterations of the genomic DNA sequence were introduced during PCR amplification or cloning. Single alanine mutations Y36A, D46A, Y49A, D50A, and K113A were introduced into the MimiLIG gene via two-stage PCR overlap extension using pET28b-His_{10}-Smt3-MimiLIG as the template for the first stage PCR reaction. *Bam*HI fragments of the mutated second stage PCR products were inserted into pET28b-His_{10}-Smt3. The CΔ336 and CΔ79 deletion mutants, encoding MimiLIG-(1–300) and MimiLIG-(1–557), were constructed by PCR amplification of the gene with antisense-strand primers that

introduced stop codons in lieu of the codons for Val301 or Glu558, respectively, and a *Bam*HI site immediately 3′ of the new stop codon. *Bam*HI fragments containing the truncated genes were inserted into pET28b-His_{10}-Smt3 vector. The DNA inserts of the resulting plasmids were sequenced to confirm the presence of the desired alanine mutations or truncated ORFs and exclude the acquisition of unwanted coding changes during amplification and cloning.

Recombinant MimiLIG

The pET28b-His_{10}-Smt3-MimiLIG plasmids were transformed into *E. coli* BL21 (DE3)-RIL. Cultures (500 ml) derived from single transformants were grown at 37 °C in Luria-Bertani medium containing 50 μg/ml kanamycin and 12.5 μg/ml chloramphenicol until the A_{600} reached 0.6. The cultures were adjusted to 0.5 mM isopropyl-1-thio-β-D-galactopyranoside and 2% (v/v) ethanol and placed on ice for 2 h, after which incubation was continued for 20 h at 17 °C with constant shaking. The cells were harvested by centrifugation and the pellets stored at −80 °C. All subsequent steps were performed at 4 °C. Thawed bacteria were resuspended in 25 ml of buffer A (50 mM Tris–HCl, pH 7.5, 500 mM NaCl, 10% glycerol). Phenylmethylsulfonyl fluoride and lysozyme were added to final concentrations of 250 μM and 100 μg/ml, respectively. After 30 min, Triton X-100 was added to a final concentration of 0.1% and the lysate was sonicated to reduce viscosity. Insoluble material was removed by centrifugation for 45 min at 16,000 rpm in a Sorvall SS34 rotor. The soluble extract was mixed for 30 min with 2 ml of Ni^{2+}-nitrilotriacetic acid-agarose resin (Qiagen) that had been pre-equilibrated with buffer A. The resin was recovered by centrifugation, resuspended in buffer A, and then poured into a column and washed with 35 ml of buffer A containing 10 mM imidazole. Bound material was eluted with 500 mM imidazole in buffer A. The eluate was dialyzed against buffer B (50 mM Tris–HCl, pH 7.5, 200 mM NaCl, 10% glycerol) containing 1 mM dithiothreitol (DTT) and 0.01% Triton X-100. The His_{10}-Smt3-tag was removed by treatment of the recombinant protein with Ulp1, an Smt3-specific protease (Mossessova and Lima, 2000), for 15 min on ice at a Ulp1: MimiLIG ratio of 1:1000. The digests were applied to 1-ml columns of Ni-agarose equilibrated with buffer B. The tag-free MimiLIG proteins were recovered in the flow-through fractions, which were stored at −80 °C. Protein concentrations were determined by using the BioRad dye reagent with BSA as the standard.

Glycerol gradient sedimentation

An aliquot (50 μg) of the tag-free wild-type MimiLIG was mixed with catalase (40 μg), ovalbumin (40 μg), and cytochrome *c* (40 μg). The mixture was applied to a 5-ml 15–30% glycerol gradient containing 50 mM Tris–HCl (pH 8.0), 500 mM NaCl, 2 mM DTT, 1 mM EDTA, and 0.05% Triton X-100. The gradient was centrifuged in a Sorvall SW55 rotor at 50,000 rpm for 17 h at 4 °C. Fractions (~0.19 ml) were collected from the bottom of the tube.

Nick ligation assay

Reaction mixtures (20 μl) containing 50 mM Tris–HCl (pH 7.5), 10 mM $(NH_4)_2SO_4$, 5 mM DTT, 5 mM $MgCl_2$, 1 pmol nicked duplex DNA substrate (shown in Fig. 2B, with the ^{32}P-labeled phosphate at the nick indicated by p), NAD^+ or ATP as specified, and MimiLIG as specified were incubated at 37 °C. The reactions were quenched with an equal volume of 95% formamide, 20 mM EDTA. The samples were heat-denatured, and aliquots (15 μl) were analyzed by electrophoresis through a 15-cm 17% polyacrylamide gel containing 7 M urea in TBE (90 mM Tris borate, 2.5 mM EDTA). The products were visualized by autoradiography and quantified by scanning the gel with a Fujix BAS2500 imager.

Adenylyltransferase activity

Reaction mixtures (20 μl) containing 50 mM Tris–HCl (pH 7.5), 5 mM DTT, 5 mM $MgCl_2$, 1.1 μM [^{32}P-adenylate]-NAD^+ (PerkinElmer Life Sciences), and 8 pmol of wild-type or mutated MimiLIG were incubated at 37 °C for 10 min. The reactions were quenched by adding SDS to 2% final concentration, and the products were analyzed by SDS-PAGE. The ligase–[^{32}P]AMP adduct was visualized by autoradiography and quantified with a Fujix BAS2500 imager.

Ligation at a preadenylylated nick

The nicked DNA–adenylylate substrate is depicted in Fig. 2D. The ^{32}P-labeled 12-mer AppDNA strand was prepared as described previously (Nandakumar and Shuman, 2005) and annealing to the complementary 24-mer and a 12-mer 3′-OH acceptor strand at a molar ratio of 1:2:5. AppDNA ligation reaction mixtures (20 μl) containing 50 mM Tris–HCl (pH 7.5), 5 mM DTT, 5 mM $MgCl_2$, 200 fmol ^{32}P-labeled nicked DNA–adenylylate, and 1 pmol of wild-type or mutated MimiLIG proteins were incubated at 37 °C for 5 min. The reactions were quenched with an equal volume of 95% formamide, 20 mM EDTA. The products were resolved by TBE–Urea PAGE as described above, visualized by autoradiography, and quantified with a Fujix BAS2500 imager.

References

Akey, D., Martins, A., Aniukwu, J., Glickman, M.S., Shuman, S., Berger, J.M., 2006. Crystal structure and nonhomologous end joining function of the ligase component of *Mycobacterium* DNA ligase D. J. Biol. Chem. 281, 13412–13423.

Becker, A., Lyn, G., Gefter, M., Hurwitz, J., 1967. The enzymatic repair of DNA: characterization of phage-induced sealase. Proc. Natl. Acad. Sci. U.S.A. 58, 1996–2003.

Benarroch, D., Claverie, J.M., Raoult, D., Shuman, S., 2005. Characterization of mimivirus DNA topoisomerase IB suggests horizontal gene transfer between eukaryal viruses and bacteria. J. Virol. 80, 314–321.

Cheng, C., Shuman, S., 1997. Characterization of an ATP-dependent DNA ligase encoded by *Haemophilus influenzae*. Nucleic Acids Res. 25, 1369–1375.

Claverie, J.M., Ogata, H., Audic, S., Abergel, C., Suhre, K., Fournier, P.E.,

2006. Mimivirus and the emerging concept of "giant" virus. Virus Res. 117, 133–144.

Fabrega, C., Shen, V., Shuman, S., Lima, C.D., 2003. Structure of an mRNA capping enzyme bound to the phosphorylated carboxyl-terminal domain of RNA polymerase II. Mol. Cell 11, 1549–1561.

Feng, H., Parker, J.M., Lu, J., Cao, W., 2004. Effects of deletion and site-directed mutations on ligation steps of NAD^+-dependent DNA ligase: a biochemical analysis of BRCA1 C-terminal domain. Biochemistry 43, 12648–12659.

Gajiwala, K., Pinko, C., 2004. Structural rearrangement accompanying NAD^+ synthesis within a bacterial DNA ligase crystal. Structure 12, 1449–1459.

Gong, C., Martins, A., Bongiorno, P., Glickman, M., Shuman, S., 2004. Biochemical and genetic analysis of the four DNA ligases of mycobacteria. J. Biol. Chem. 279, 20594–20606.

Gottesman, M.M., Hicks, M.L., Gellert, M., 1973. Genetics and function of DNA ligase in *Escherichia coli*. J. Mol. Biol. 77, 531–547.

Greub, G., Raoult, D., 2004. Microorganisms resistant to free-living amoebae. Clin. Microbiol. Rev. 17, 413–433.

Håkansson, K., Doherty, A.J., Shuman, S., Wigley, D.B., 1997. X-ray crystallography reveals a large conformational change during guanyl transfer by mRNA capping enzymes. Cell 89, 545–553.

Hammond, J.M., Kerr, S.M., Smith, G.L., Dixon, L.K., 1992. An African swine fever virus gene with homology to DNA ligases. Nucleic Acids Res. 20, 2667–2671.

Harvey, C.L., Gabriel, T.F., Wilt, E.M., Richardson, C.C., 1971. Enzymatic breakage and rejoining of deoxyribonucleic acid: synthesis and properties of the deoxyribonucleic acid adenylate in the phage T4 ligase reaction. J. Biol. Chem. 246, 4523–4530.

Hertveldt, K., Lavigne, R., Pleteneva, E., Sernova, N., Kurochkina, L., Korchevskii, R., Robben, J., Mesyanzhinov, V., Krylov, V.N., Volckaert, G., 2005. Genome comparison of *Pseudomonas aeruginosa* large phages. J. Mol. Biol. 354, 536–545.

Ho, C.K., Van Etten, J.L., Shuman, S., 1997. Characterization of an ATP-dependent DNA ligase encoded by *Chlorella* virus PBCV-1. J. Virol. 71, 1931–1937.

Jakob, N.J., Müller, K., Bahr, U., Darai, G., 2001. Analysis of the first complete DNA sequence of an invertebrate iridovirus: coding strategy of the genome of Chilo iridescent virus. Virology 286, 182–196.

Jeon, H.J., Shin, H.J., Hoe, J.J., Kim, H.S., Suh, S.K., Kwon, S.W., 2004. Mutational analyses of the thermostable NAD^+-dependent DNA ligase from *Thermus filiformis*. FEMS Microbiol. Lett. 237, 111–118.

Kaczmarek, F.S., Zaniewski, R.P., Gootz, T.D., Danley, D.E., Mansour, M.N., Griffor, M., Kamath, A.V., Cronan, M., Mueller, J., Sun, D., Martin, P.K., Benton, B., McDowell, L., Biek, D., Schmid, M.B., 2001. Cloning and functional characterization of an NAD^+-dependent DNA ligase from *Staphylococcus aureus*. J. Bacteriol. 183, 3016–3024.

Keppetipola, N., Shuman, S., 2005. Characterization of a thermophilic ATP-dependent DNA ligase from the euryarchaeon *Pyrococcus horikoshii*. J. Bacteriol. 187, 6902–6908.

Kerr, S.M., Smith, G.L., 1989. Vaccinia virus encodes a polypeptide with DNA ligase activity. Nucleic Acids Res. 17, 9039–9050.

Konrad, E.B., Modrich, P., Lehman, I.R., 1973. Genetic and enzymatic characterization of a conditional lethal mutant of *Escherichia coli* K12 with a temperature-sensitive DNA ligase. J. Mol. Biol. 77, 519–529.

Lamarche, B.J., Showalter, A.K., Tsai, M.D., 2005. An error-prone viral DNA ligase. Biochemistry 44, 8408–8417.

Lee, J.Y., Chang, C., Song, H.K., Moon, J., Yang, J., Kim, H.K., Kwon, S. T., Suh, S.W., 2000. Crystal structure of NAD^+-dependent DNA ligase: modular architecture and functional implications. EMBO J. 19, 1119–1129.

Lehman, I.R., 1974. DNA ligase: structure, mechanism, and function. Science 186, 790–797.

Lim, J.H., Choi, J., Kim, W., Ahn, B.Y., Han, Y.S., 2001. Mutational analyses of *Aquifex pyrophilus* DNA ligase define essential domains for self-adenylation and DNA binding. Arch. Biochem. Biophys. 388, 253–260.

Lu, J., Tong, J., Feng, H., Huang, J., Afonso, C.L., Rock, D.L., Barany, F., Cao, W., 2004. Unique ligation properties of eukaryotic NAD^+-dependent DNA ligase from *Melanoplus sanguinipes* entomopoxvirus. Biochim. Biophys. Acta 1701, 37–48.

Luo, J., Barany, F., 1996. Identification of essential residues in *Thermus thermophilus* DNA ligase. Nucleic Acids Res. 24, 3079–3085.

Martin, I.V., MacNeill, S.A., 2002. ATP-dependent DNA ligases. Genome Biol. 3, 3005.1–3005.7.

Mossessova, E., Lima, C.D., 2000. Ulp1-SUMO crystal structure and genetic analysis reveal conserved interactions and a regulatory element essential for cell growth in yeast. Mol. Cell 5, 865–876.

Nandakumar, J., Shuman, S., 2005. Dual mechanisms whereby a broken RNA end assists the catalysis of its repair by T4 RNA ligase 2. J. Biol. Chem. 280, 23484–23489.

Odell, M., Sriskanda, V., Shuman, S., Nikolov, D.B., 2000. Crystal structure of eukaryotic DNA ligase–adenylate illuminates the mechanism of nick sensing and strand joining. Mol. Cell 6, 1183–1193.

Olivera, B.M., Lehman, I.R., 1967. Diphosphopyridine nucleotide: a cofactor for the polynucleotide-joining enzyme from *Escherichia coli*. Proc. Natl. Acad. Sci. U.S.A. 57, 1700–1704.

Park, U.E., Olivera, B.M., Hughes, K.T., Roth, J.R., Hillyard, D.R., 1989. DNA ligase and the pyridine cycle in *Salmonella typhimurium*. J. Bacteriol. 171, 2173–2180.

Pascal, J.M., O'Brien, P.J., Tomkinson, A.E., Ellenberger, T., 2004. Human DNA ligase I completely encircles and partially unwinds nicked DNA. Nature 432, 473–478.

Pearson, M.N., Rohrmann, G.F., 1998. Characterization of a baculovirus-encoded ATP-dependent DNA ligase. J. Virol. 72, 9142–9149.

Petit, M.A., Ehrlich, S.D., 2000. The NAD-dependent ligase encoded by yerG is an essential gene of *Bacillus subtilis*. Nucleic Acids Res. 28, 4642–4648.

Raoult, D., Audic, S., Robert, C., Abergel, C., Renesto, P., Ogata, H., La Scola, B., Suzan, M., Claverie, J.M., 2004. The 1.2-megabase genome sequence of Mimivirus. Science 306, 1344–1350.

Sekiguchi, J., Shuman, S., 1997. Nick sensing by DNA ligase requires a 5′ phosphate at the nick and occupancy of the adenylate binding site on the enzyme. J. Virol. 71, 9679–9684.

Shuman, S., 1995. Vaccinia DNA ligase: specificity, fidelity, and inhibition. Biochemistry 34, 16138–16147.

Shuman, S., Ru, X., 1995. Mutational analysis of vaccinia DNA ligase defines residues essential for covalent catalysis. Virology 211, 73–83.

Shuman, S., Lima, C.D., 2004. The polynucleotide ligase and RNA capping enzyme superfamily of covalent nucleotidyltransferases. Curr. Opin. Struct. Biol. 14, 757–764.

Singleton, M.R., Håkansson, K., Timson, D.J., Wigley, D.B., 1999. Structure of the adenylation domain of an NAD+-dependent DNA ligase. Structure 7, 35–42.

Sriskanda, V., Shuman, S., 1998. *Chlorella* virus DNA ligase: nick recognition and mutational analysis. Nucleic Acids Res. 26, 525–531.

Sriskanda, V., Shuman, S., 2001. A second NAD^+-dependent DNA ligase (LigB) in *Escherichia coli*. Nucleic Acids Res. 29, 4930–4934.

Sriskanda, V., Shuman, S., 2002a. Role of nucleotidyl transferase motifs I, III and IV in the catalysis of phosphodiester bond formation by *Chlorella virus* DNA ligase. Nucleic Acids Res. 30, 903–911.

Sriskanda, V., Shuman, S., 2002b. Role of nucleotidyl transferase motif V in strand joining by *Chlorella virus* DNA ligase. J. Biol. Chem. 277, 9661–9667.

Sriskanda, V., Shuman, S., 2002c. Conserved residues in domain Ia are required for the reaction of *Escherichia coli* DNA ligase with NAD^+. J. Biol. Chem. 277, 9695–9700.

Sriskanda, V., Schwer, B., Ho, C.K., Shuman, S., 1999. Mutational analysis of *Escherichia coli* DNA ligase identifies amino acids required for nick-ligation in vitro and for in vivo complementation of the growth of yeast cells deleted for CDC9 and LIG4. Nucleic Acids Res. 27, 3953–3963.

Sriskanda, V., Kelman, Z., Hurwitz, J., Shuman, S., 2000. Characterization of an ATP-dependent DNA ligase from the thermophilic archaeon *Methanobacterium thermoautotrophicum*. Nucleic Acids Res. 28, 2221–2228.

Sriskanda, V., Moyer, R.W., Shuman, S., 2001. NAD^+-dependent DNA ligase encoded by a eukaryotic virus. J. Biol. Chem. 276, 36100–36109.

Srivastiva, S.K., Tripathi, R.P., Ramachandran, R., 2005. NAD^+-dependent DNA ligase (Rv3014c) from *Mycobacterium tuberculosis*: crystal structure of the adenylation domain and identification of novel inhibitors. J. Biol. Chem. 280, 30273–30281.

Subramanya, H.S., Doherty, A.J., Ashford, S.R., Wigley, D.B., 1996. Crystal structure of an ATP-dependent DNA ligase from bacteriophage T7. Cell 85, 607–615.

Timson, D.J., Wigley, D.B., 1999. Functional domains of an NAD^+-dependent DNA ligase. J. Mol. Biol. 285, 73–83.

Wang, J., Jiang, Y., Vincent, M., Sun, Y., Yu, H., Wang, J., Bao, Q., Kong, H., Hu, S., 2005. Complete genome of bacteriophage T5. Virology 332, 45–65.

Weiss, B., Richardson, C.C., 1967. Enzymatic breakage and joining of deoxyribonucleic acid: repair of single-strand breaks in DNA by an enzyme system from *Escherichia coli* infected with T4 bacteriophage. Proc. Natl. Acad. Sci. U.S.A. 57, 1021–1028.

Weiss, B., Thompson, A., Richardson, C.C., 1968. Enzymatic breakage and rejoining of deoxyribonucleic acid: properties of the enzyme–adenylate intermediate in the polynucleotide ligase reaction. J. Biol. Chem. 246, 4523–4530.

Wilkinson, A., Day, J., Bowater, R., 2001. Bacterial DNA ligases. Mol. Microbiol. 40, 1241–1248.

Wilkinson, A., Smith, A., Bullard, D., Lavesa-Curto, M., Sayer, H., Bonner, A., Hemmings, A., Bowater, R., 2005. Analysis of ligation and DNA binding by *Escherichia coli* DNA ligase (LigA). Biochim. Biophys. Acta 1749, 113–122.

Zhao, A., Gray, F.C., MacNeill, S.A., 2006. ATP- and NAD^+-dependent DNA ligases share an essential function in the halophilic archaeon *Haloferax volcanii*. Mol. Microbiol. 59, 743–752.

Zhu, H., Shuman, S., 2005. Structure-guided mutational analysis of the nucleotidyltransferase domain of *Escherichia coli* NAD^+-dependent DNA ligase (LigA). J. Biol. Chem. 280, 12137–12144.

Zimmerman, S.B., Little, J.W., Oshinsky, C.K., Gellert, M., 1967. Enzymatic joining of DNA strands: a novel reaction of diphosphopyridine nucleotide. Proc. Natl. Acad. Sci. U.S.A. 57, 1841–1848.